

MOC-RVQ: Multilevel Codebook-assisted Digital Generative Semantic Communication

Yingbin Zhou¹ Yaping Sun^{2,1} Guanying Chen¹ Xiaodong Xu^{3,2}

Hao Chen² Binhong Huang² Shuguang Cui^{1,2} Ping Zhang^{3,2}

¹FNii and SSE, The Chinese University of Hong Kong, Shenzhen, China

²Peng Cheng Laboratory, Shenzhen, China

³Beijing University of Posts and Telecommunications, Beijing, China

Abstract—Vector quantization-based image semantic communication systems have successfully boosted transmission efficiency, but face a challenge with conflicting requirements between codebook design and digital constellation modulation. Traditional codebooks need a wide index range, while modulation favors few discrete states. To address this, we propose a multilevel generative semantic communication system with a two-stage training framework. In the first stage, we train a high-quality codebook, using a multi-head octonary codebook (MOC) to compress the index range. We also integrate a residual vector quantization (RVQ) mechanism for effective multilevel communication. In the second stage, a noise reduction block (NRB) based on Swin Transformer is introduced, coupled with the multilevel codebook from the first stage, serving as a high-quality semantic knowledge base (SKB) for generative feature restoration. Experimental results highlight MOC-RVQ's superior performance over methods like BPG or JPEG, even without channel error correction coding.

Index Terms—vector quantization, generative semantic communication, two-stage training, semantic knowledge base

I. INTRODUCTION

Traditional communication systems focus on the bit/symbol-level transmission, where the receiver seeks to minimize bit/symbol transmission errors to recover digital media [1]. This allows the design of communication system architecture to be separated from the vast and complex content of media. As a result, bit/symbol-based transmission has long been the prevailing paradigm in traditional communication systems.

Recently, propelled by the rapid development of deep learning technology, a new intelligent transmission paradigm known as semantic communication is gradually gaining prominence. In contrast to traditional transmission, semantic communication aims for the transmission of semantic fidelity [2]. For example, Dai *et al.* [3] integrate the nonlinear transform as a robust prior to efficiently extract source semantic features. Yang *et al.* [4] introduce a deep joint source-channel coding (JSCC) strategy designed for the transmission of images in wireless communication. Sun *et al.* [5] design a multi-level semantic coding and feature transmission mechanism powered by semantic knowledge base. However, these works suffer from efficiency issues, due to the high dimension of latent representation of raw data.

One solution to achieve a compact representation is vector quantization (VQ) technique [6]. Generally, VQ transforms semantic features into a series of indices, providing a more compact format that can be further converted into bits for

transmission, then the receiver utilizes the received indices to reconstruct the semantic features through a pre-established learned codebook. Ultimately, the raw data or the task-oriented information can be decoded from these reconstructed semantic features. Nemati *et al.* [7] delve into the characteristics of VQ-VAE and adapt its training process to formulate a robust JSCC scheme against noisy wireless channels. Fu *et al.* [8] design a CNN-based transceiver to extract multi-scale semantic features and incorporate multi-scale semantic embedding spaces to facilitate feature quantization. To improve semantic representation in digital transmission under resource limitations, Guo *et al.* [9] introduce a novel non-linear quantization module with trainable levels for efficient feature extraction.

However, methods above suffer the following two issues:

- **Incompatible issue** arises from the disparity between conventional vector quantization and digital constellation modulation. The former, aimed at achieving optimal image representation, employs a learnable codebook with a wide range of code indices. In contrast, the latter is more inclined to handle fewer states (e.g., 16-QAM, 64-QAM, etc.). While it is conceivable to regroup bits representing indices to align with modulation, such an adjustment also disrupts the explicit relationship between indices and constellation points. Note that this explicit relationship is crucial for preserving the local semantic relationship of the underlying neighbour code vectors, which directly affects the quality of reconstructed image.
- **Mismatch issue** occurs in the local relationship between code indices and code vectors, which renders vector quantization-based semantic communication systems susceptible to channel noise. For instance, while the difference between index "1" and index "2" is 1, the distance between the underlying code vectors of index "1" and index "2" can be substantial. This mismatch may lead to errors in decoding and, consequently, degrade the overall performance of the communication system.

To tackle the incompatible issue, we introduce MOC-RVQ with two stage training framework. In Stage 1, we introduce (1) MOC, a variant of vector quantizer by constructing a *multi-head octonary codebook (MOC)* to compress discrete states to a limit of 8, allowing for a direct match with 64-QAM. (2) RVQ, a multi-level semantic transmission mechanism based

on residual vector quantization (RVQ), which is helpful to compensate the negative effect of the quantization noise [10], [11]. These two components are integrated to form MOC-RVQ. Subsequently, in Stage 2, we propose a noise reduction block (NRB) and feature requantization to achieve generative feature restoration. **For the mismatch issue**, we adopt a heuristic codebook reordering algorithm, which is aimed at minimizing the semantic distance between underlying code vectors with nearby indices.

Overall, the main contributions are summarized as follows:

- We point out two inherent shortcomings of the existing VQ-based semantic communication system and propose a novel two-stage framework.
- We introduce MOC-RVQ to align with the property of digital constellation modulation. Then noise reduction block (NRB) based on Swin Transformer and feature requantization are incorporated for generative semantic reconstruction.
- We propose a codebook reordering algorithm, inspired by Gray code mapping, to alleviate the discrepancy in the local relationships among code vectors with nearby indices. This algorithm serves to enhance the overall robustness of the system against channel noise.

II. SYSTEM MODEL

In this section, we present a general VQ-based semantic communication framework, which we will subsequently extend to our two-stage framework in Section III. The core pipeline is depicted in Fig. 1. In this setup, both the transmitter and receiver employ a pre-established semantic codebook as semantic knowledge base (SKB) to achieve an efficient process for compressing and recovering of semantic features, ultimately leading to a reduction in communication overhead.

A. Transmitter

Given an input image $\mathbf{I} \in \mathbb{R}^{H \times W \times 3}$, the semantic encoder E (served as understanding knowledge base) is employed initially to transform \mathbf{I} into a semantic feature $\mathbf{z} \in \mathbb{R}^{h \times w \times n_q}$. Subsequently, each grid feature $\mathbf{z}^{(i,j)} \in \mathbb{R}^{n_q}$ is substituted with the nearest entry in the learnable codebook $\mathcal{C} = \{\mathbf{e}_k \in \mathbb{R}^{n_q}\}_{k=0}^N$. This substitution yields the quantized feature \mathbf{z}_q along with the corresponding code index sequence $\mathbf{s} \in \{0, 1, \dots, N-1\}^{h \cdot w}$, by the following equations:

$$\mathbf{z}_q^{(i,j)} = \mathbf{Q}(\mathbf{z}^{(i,j)}) = \mathbf{e}_{\mathbf{s}^{(i,j)}} \in \mathbb{R}^{n_q}, \quad (1)$$

$$\mathbf{s}^{(i,j)} = \underset{k}{\operatorname{argmin}} \left\| \mathbf{z}^{(i,j)} - \mathbf{e}_k \right\| \in \{0, 1, \dots, N-1\}, \quad (2)$$

where $\mathbf{Q}(\cdot)$ is a quantization operation that maps the continuous encoded grid feature $\mathbf{z}^{(i,j)}$ into the quantized form $\mathbf{z}_q^{(i,j)}$ by looking up the closest codebook entry \mathbf{e}_k . Note that the code index sequence \mathbf{s} can be served as a compact equivalent representation of the quantized feature \mathbf{z}_q . This implies that transmitting only the code index sequence \mathbf{s} can effectively reduce communication overhead. Following decimal to binary transform and digital constellation modulation, \mathbf{s} is converted

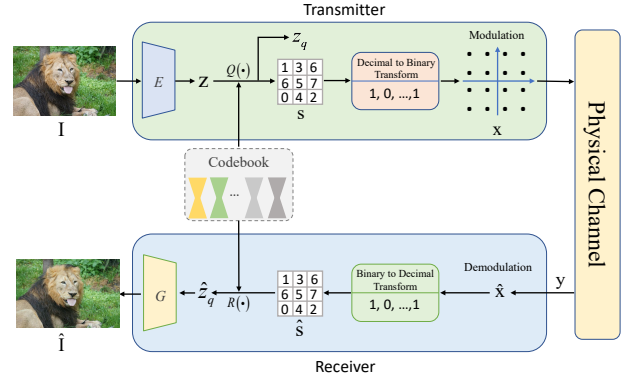


Fig. 1. An essential structure for VQ-based semantic communication with the presence of a stochastic physical channel.

as a transmitted complex signal $\mathbf{x} \in \mathbb{C}^{B \times 1}$, where B represents the length of the transmitted signal.

B. Physical Channel

To simplify channel modeling without sacrificing representativeness, we adopt the additive white Gaussian noise (AWGN) as follows:

$$\mathbf{y} = \mathbf{x} + \mathbf{w}, \quad (3)$$

where $\mathbf{y} \in \mathbb{C}^{B \times 1}$ represents the received complex signal. The AWGN \mathbf{w} has i.i.d elements with zero mean and variance σ^2 .

C. Receiver

After demodulation of the received signal \mathbf{y} , the receiver obtains $\hat{\mathbf{x}}$. Subsequently, the binary to decimal transform retrieves the indices $\hat{\mathbf{s}}$ from $\hat{\mathbf{x}}$ (Note that $\hat{\mathbf{s}}$ can be served as a prompt in a large language model, we utilize it to generate high quality reconstructed image). By selecting the corresponding embedding vectors from the codebook \mathcal{C} , the receiver reconstructs the semantic feature tensor $\hat{\mathbf{z}}_q$, we define this process as semantic feature retrieval $\mathbf{R}(\cdot)$. Finally, leveraging this retrieval semantic information, the semantic decoder G (served as generative knowledge base) generates the reconstructed image $\hat{\mathbf{I}}$.

III. THE PROPOSED METHOD

In this section, we introduce a novel two-stage framework to enhance vector quantization-based semantic communication. Subsequently, we delve into the description of codebook reordering, an algorithm employed to minimize the mismatch between local relationships of code indices and code vectors.

A. Stage 1: Pretraining of MOC-RVQ

The primary objective of Stage 1 is to train a high-quality encoder/decoder model and codebook without any channel noise, aiming for a compact representation of images. As depicted in Fig. 2 (Left), in Stage 1, an input image $\mathbf{I} \in \mathbb{R}^{H \times W \times 3}$ is initially fed into the encoder E to yield a continuous semantic feature $\mathbf{z} \in \mathbb{R}^{h \times w \times n_q}$. Subsequently,

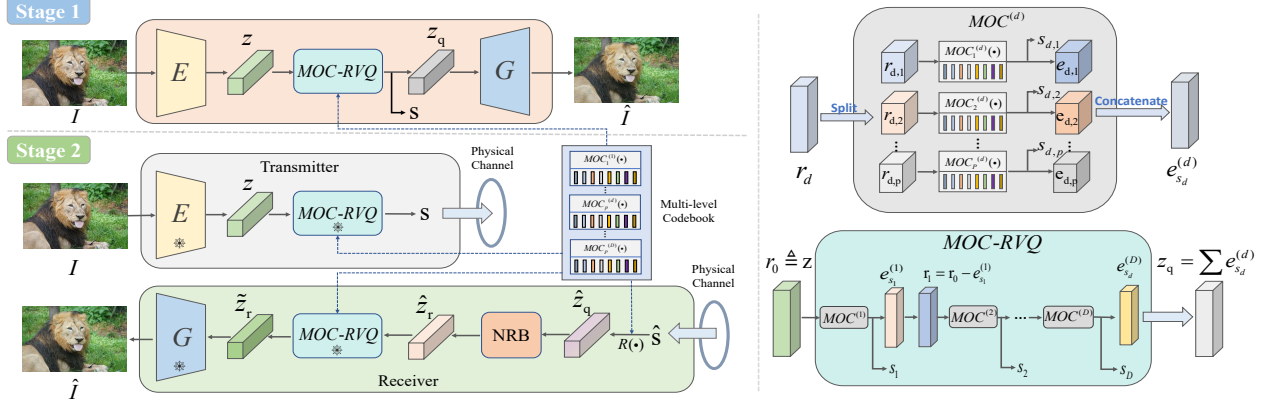


Fig. 2. **Left:** The proposed two-stage framework. In Stage 1, we initially pretrain MOC-RVQ and other model components to generate compact representation of high-resolution image. Then the noise reduction block (NRB) is finetuned in Stage 2 to achieve feature restoration. **Right:** The architecture of the proposed MOC and MOC-RVQ. In MOC, each residual feature \mathbf{r}_d is first divided into several heads, then the 8-state codebook is employed to quantize each head feature, and finally these features are concatenated together to form a single quantized feature. In MOC-RVQ, feature are recursive quantized by MOC to produce residual features and the corresponding code indices. Note that the output of MOC-RVQ is a summation over all quantized features $\mathbf{e}_{s_d}^{(d)}$.

the MOC-RVQ layer quantizes this feature, resulting in the quantized feature \mathbf{z}_q and an associated code indices sequence $\mathbf{s} \in \{0, \dots, N-1\}^{h \cdot w \cdot P \cdot D}$. Here, P and D represent the number of heads and the level of quantizations respectively, and N is set to 8 to align with the few states prior of 64-QAM. Finally, the quantized feature \mathbf{z}_q is fed into the decoder G to reconstruct the image as $\hat{\mathbf{I}}$.

The detailed designs of multi-head octonary codebook (MOC) and MOC-RVQ are illustrated in Fig. 2 (Right), and their functionality can be described as follows:

a) *MOC*: Given a quantization level d , each residual feature $\mathbf{r}_d \in \mathbb{R}^{h \times h \times n_q}$ is initially divided into several heads $\mathbf{r}_{d,i} \in \mathbb{R}^{h \times h \times n_q/P}$ (typically set P to 4 by default). Subsequently, an 8-state codebook is employed to quantize each head, yielding head-wise quantized features $\mathbf{e}_{d,i}$. These quantized features are then concatenated to form a single quantized feature $\mathbf{e}_{s_d}^{(d)}$. This distinctive codebook design for digital constellation modulation is termed as the multi-head octonary codebook (MOC). In contrast to conventional codebook with size K , our proposed MOC dramatically expands the feature matching space, generating N^P discrete states through the combination of each head state.

b) *MOC-RVQ*: By replacing the naive quantizer with MOC, we introduce a multilevel semantic transmission mechanism based on residual vector quantization (RVQ) to counteract potential adverse effects resulting from the quantization process, ultimately further enhances the system's reconstruction performance. Specifically, with a default quantization level D set to 4, the semantic feature \mathbf{z} undergoes recursive quantization to produce residual code indices as follows:

$$\text{MOC-RVQ}(\mathbf{z}) = (\mathbf{s}_1, \dots, \mathbf{s}_D), \quad (4)$$

where $\mathbf{s}_d \in \{0, \dots, N-1\}^{h \cdot w \cdot P}$ represents the code indices of \mathbf{z} at level d , and P denotes the number of heads. Given an

initial residual $\mathbf{r}_0 = \mathbf{z}$, the recursive process computes indices \mathbf{s}_d and the next residual \mathbf{r}_d as follows:

$$\mathbf{s}_d = \text{MOC}^{(d)}(\mathbf{r}_{d-1}), \quad (5)$$

$$\mathbf{r}_d = \mathbf{r}_{d-1} - \mathbf{e}_{s_d}^{(d)}, \quad (6)$$

where $\text{MOC}^{(d)}(\cdot)$ is the d -th MOC quantizer, and $\mathbf{e}^{(d)}$ is the corresponding codebook embedding. The final quantized result of MOC-RVQ is obtained by $\mathbf{z}_q = \sum_{d=1}^D \mathbf{e}_{s_d}^{(d)}$.

c) *Training Objectives*: To train the proposed model, several loss functions are introduced into our method. Since the feature quantization operation is non-differentiable, we adopt the approach from [12] by copying gradients from G to E during backpropagation. This enables end-to-end training of the encoder/decoder model and codebook, guided by the following objective function:

$$\mathcal{L}'_{VQ}(E, G, \mathcal{C}) = \|\hat{\mathbf{I}} - \mathbf{I}\|_1 + \sum_{d,h} \|\text{sg}[\mathbf{r}_{d,h}] - \mathbf{e}_{d,h}\|_2^2, \quad (7)$$

where $\text{sg}[\cdot]$ represents the stop-gradient operation, and $\mathbf{r}_{d,h}$ and $\mathbf{e}_{d,h}$ denote the d -th quantization of the h -th head of residual and quantized features, respectively.

To enhance texture restoration, a semantic guidance loss, as proposed in [13], is also introduced as a regularization term:

$$\mathcal{L}_{VQ} = \mathcal{L}'_{VQ} + \gamma \|\text{CONV}(\mathbf{z}) - \phi(\mathbf{I})\|_2^2, \quad (8)$$

where $\text{CONV}(\cdot)$ denotes a 1×1 convolution layer to align the dimensions of \mathbf{z} , ϕ represents the pretrained VGG19 model, and γ is set to 0.1. Additionally, in accordance with [12], perceptual loss and adversarial loss are employed for model pretraining.

B. Stage 2: Finetuning for Noise Reduction

Since Stage 1 is trained end-to-end without accounting for channel noise, leading to suboptimal reconstructed results in the presence of noise, we integrate a noise reduction block (NRB) based on a stack of residual Swin Transformer layers,

as mentioned in [13] into decoder G to conduct generative image reconstruction.

Building upon the pretrained model and codebook from Stage 1, as depicted in Fig. 2 (Left), Stage 2 introduces an physical communication channel module (refer to Section II-B for details) between transmitter and receiver for physical channel simulation. Then the noise reduction block is incorporated after the retrieval feature $\hat{\mathbf{z}}_q$ to refine semantic features, yielding the refined semantic feature $\hat{\mathbf{z}}_r$.

a) *Feature Requantization*: To further enhance the quality of $\hat{\mathbf{z}}_r$, we propose requantizing it to obtain $\tilde{\mathbf{z}}_r$, formulated as follows:

$$\tilde{\mathbf{z}}_r = \mathcal{MOC} - \mathcal{RVQ}(\hat{\mathbf{z}}_r). \quad (9)$$

The intuition behind this lies in the fact that MOC is trained in the absence of any noise, establishing itself as a high-quality semantic knowledge base to inject high quality prior for better feature restoration.

b) *Training Objectives*: For NRB finetuning, we generate the noiseless quantized semantic feature of image \mathbf{I} through $\mathbf{z}_q = \mathcal{MOC}(E(\mathbf{I}))$ as the ground-truth feature. This ground-truth feature is then used to calculate the Gram matrix loss and L2 loss for the refined semantic feature $\hat{\mathbf{z}}_r$ by the following formula:

$$\mathcal{L}_{NR} = \|\psi(\hat{\mathbf{z}}_r) - \psi(\text{sg}[\mathbf{z}_q])\|_2^2 + \alpha \|\hat{\mathbf{z}}_r - \text{sg}[\mathbf{z}_q]\|_2^2, \quad (10)$$

where $\psi(\cdot)$ is the flattened version of the Gram matrix of a given feature, and α is set to 0.25. The first term of \mathcal{L}_{NR} , also known as style loss, has been demonstrated to be effective for improved feature recovery [13]. Note that the model and codebook trained in Stage 1 remain fixed, and we only finetune the NRB for noise reduction.

C. Codebook Reordering

As discussed in Section I, a discrepancy exists in the local relationship between code indices and code vectors, rendering VQ-based semantic communication systems susceptible to channel noise. In response to this challenge, we propose a heuristic solution through the codebook reordering (CR) algorithm outlined in Algorithm 1. The algorithm systematically searches for the nearest neighbor vector within \mathcal{C} , constructing a new vector sequence, which is then assembled to form a preliminarily sorted codebook. Furthermore, to align with the design principles of Gray code mapping in digital constellation modulation, we also integrate Gray code mapping into our codebook reordering algorithm. The basic idea is to establish proximity relationships under the context of Gray code mapping. For instance, given a 3-bit Gray code sequence represented in decimals as $g = \{0, 1, 3, 2, 6, 7, 5, 4\}$, it becomes apparent that "2" and "6" are neighboring elements within the framework of Gray code mapping. Thus, it is essential to allocate two closely related code vectors to these indices.

After codebook reordering, the semantic distance between two adjacent Gray code vectors in the updated codebook \mathcal{C}^* is reduced compared to the previous disordered version. This

Algorithm 1: Codebook Reordering

input : A disordered codebook \mathcal{C} of size $N \times n_q$
output: An ordered codebook \mathcal{C}^* of size $N \times n_q$
 // Initialization
 1 $\mathcal{C}^* \leftarrow \emptyset$;
 2 $\mathbf{s}_0 \leftarrow$ mean of \mathcal{C} along dimension 0 ;
 3 **for** $i \leftarrow 1$ **to** N **do**
 4 $\mathbf{s}_i \leftarrow$ the vector closest to \mathbf{s}_{i-1} in \mathcal{C} ;
 5 Remove \mathbf{s}_i from \mathcal{C} ;
 6 Append \mathbf{s}_i to \mathcal{C}^* ;
 // Gray Code Mapping
 7 $g \leftarrow$ generate Gray code sequence of size N ;
 8 $\mathcal{C}^*[g, :] \leftarrow \mathcal{C}^*$;

addresses the issue where a small jump in the code index could lead to a significant jump in the semantic vector.

IV. EXPERIMENTS

A. Implementation Details

a) *Model and Dataset*: In accordance with Chen et al. [13], we employ a baseline autoencoder with a downsampling factor $f = 8$, indicating that the resolution of latent features is $1/f^2$ of the input resolution. To ensure effective model training, we assemble a comprehensive training set by integrating diverse datasets: DIV2K [14], Flickr2K [15], DIV8K [16], and a dataset comprising 10,000 facial images from FFHQ [17]. The generation of training patches involves the following steps: (1) extraction of non-overlapping patches with dimensions 512×512 ; (2) filtration of patches with minimal texture variation; (3) for the FFHQ dataset, a random resizing operation is applied with scale factors in the range $[0.5, 1.0]$ before cropping. For testing, we uniformly sample 25 high resolution images (with average resolution of 2012×1407) from DIV2K validation set as our test set to simulate modern image transmission scenarios.

b) *Training Details*: We employ the Adam optimizer with $\beta_1 = 0.9$ and $\beta_2 = 0.99$ for both stages, maintaining a learning rate of 0.0001 throughout the training process. The input image size is randomly cropped to 256×256 with a batch size of 16. The model pretraining stage requires approximately 3 days on 2 GeForce RTX 3090 GPUs, and the NRB finetuning stage also takes about 3 days on the same device.

B. Simulations and Discussions

In this section, we empirically demonstrate the qualitative and quantitative results of our approach, conduct model ablations, and compare our method with two state-of-the-art baselines. Note that all approaches are under 64-QAM. For channel simulation, initially, we simulate an additive white Gaussian noise (AWGN) channel with SNR varying from -5 to 30 to encompass low, medium, and high-quality channel conditions. Subsequently, we finetune our proposed NRB under this AWGN channel to enhance image reconstruction.

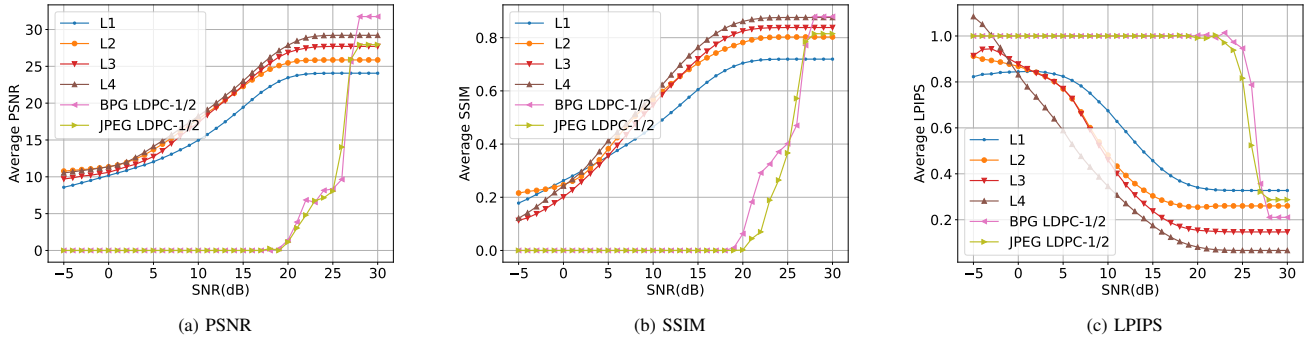


Fig. 3. Experimental comparison of methods using PSNR, SSIM, and LPIPS metrics over an additive white Gaussian noise (AWGN) channel with SNR varying from -5 to 30. L1 to L4 denote the level of quantization of our proposed MOC-RVQ, which directly determines the number of bits that need to be transmitted for communication.

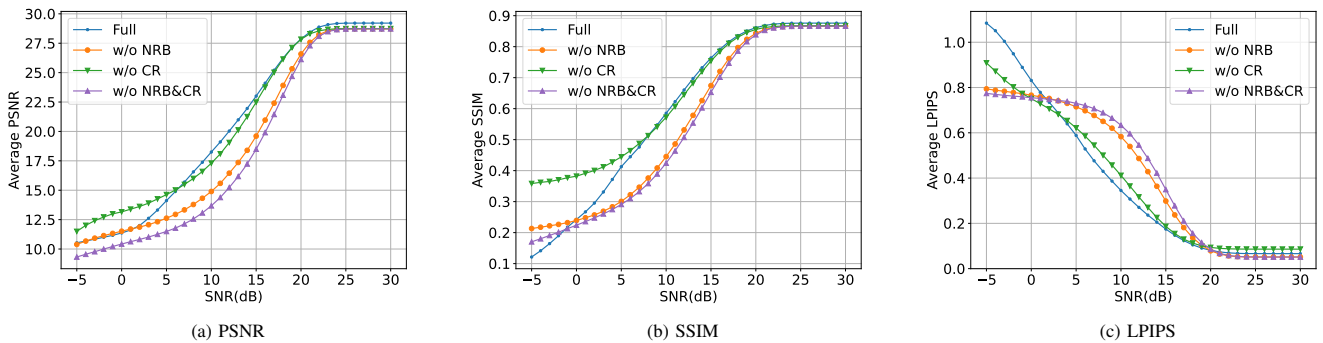


Fig. 4. Ablation study to comprehend the influence of our proposed noise reduction block (NRB) and codebook reordering (CR) algorithm. Note that all experiments are conducted on the basis of L4 transmission.

For comparison, we apply the better portable graphics (BPG [18]) and the joint picture expert group (JPEG [19]) as baselines. Notably, both of these image codec formats are susceptible to bit errors, leading to potential image format errors and decoding failures. To mitigate this, we introduce a widely used channel error correction code called Low-Density Parity-Check (LDPC) by setting the LDPC block length and bit rate as 648 bits and 1/2, respectively. Thanks to the self-restoring capability of our proposed method, we do not apply any channel error correction code, which reduces the number of transmitted bits and significantly improves the transmission efficiency of the proposed communication system.

As depicted in Fig. 3, we utilize PSNR, SSIM, and LPIPS as metrics for various methods with a similar number of transmitted symbols over the AWGN channel. LPIPS [20] is specifically introduced for evaluating the perceptual quality of generated images in semantic communication scenarios. Our proposed method exhibits remarkable robustness in deteriorating channel quality, outperforming traditional image coding even without channel error correction mechanism. This is attributed to the VQ-based semantic communication system’s independence from encoding formats, where minor bit changes do not lead to decoding failures. Additionally, the incorporation of NRB and codebook reordering further enhances the

robustness of the semantic communication system.

Figure 3 also reveals that lowering the transmission level (L4 to L1) of our model reduces the number of transmitted bits, but it also compromises reconstruction performance. Especially, we can clearly observe the gaps at different levels in LPIPS metrics, which implies that we can dynamically adjust the number of bits that need to be transmitted based on the quality of the channel and the receiver’s requirements for image quality.

In Figure 4, we present an ablation study to understand the impact of our proposed NRB and the CR algorithm. Focusing on LPIPS scores, which better capture perceptual quality, we observe the crucial role of NRB in reconstruction performance, especially under poor channel quality. Simultaneously, the proposed codebook reordering algorithm provides additional gains in image reconstruction performance.

Figure 5 illustrates the visual effect of NRB. With the assistance of NRB, even under relatively poor channel quality (SNR=5), our full model impressively reconstructs images with clear semantic meaning, which greatly expands the working conditions of VQ-based semantic communication systems.

V. CONCLUSION

We introduce MOC-RVQ, a novel two-stage framework addressing challenges in vector quantization and digital con-

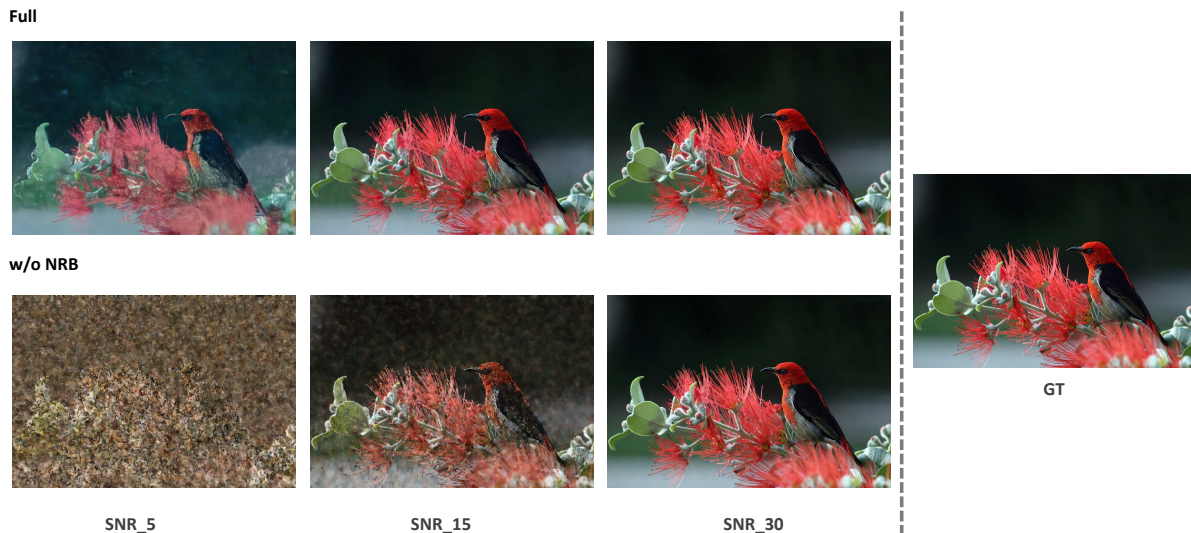


Fig. 5. Visualizing the impact of NRB across varying channel conditions. Even in poor channel quality (SNR=5), our full model impressively reconstructs images with clear semantic meaning, demonstrating the robustness of VQ-based semantic communication systems with the assistance of NRB.

stellation modulation for semantic communication systems. By incorporating a multi-head octonary codebook (MOC) to compress the index range and a residual vector quantization (RVQ) mechanism for efficient multilevel semantic communication, our approach demonstrates superior performance over existing methods like BPG and JPEG, even without channel error correction coding. The innovative two-stage model training framework, featuring a noise reduction block (NRB), enhances the system's ability to restore high-quality semantic features in the presence of channel noise. Additionally, a heuristic codebook reordering algorithm improves system robustness against channel noise, mitigating the inherent mismatch between vector quantization and digital constellation modulation. MOC-RVQ represents a significant advancement in generative semantic communication, providing a promising solution for the joint design challenges and paving the way for further exploration in intelligent communication systems.

REFERENCES

- [1] D. Huang, X. Tao, F. Gao, and J. Lu, "Deep learning-based image semantic coding for semantic communications," in *2021 IEEE Global Communications Conference (GLOBECOM)*. IEEE, 2021, pp. 1–6.
- [2] J. Bao, P. Basu, M. Dean, C. Partridge, A. Swami, W. Leland, and J. A. Hendler, "Towards a theory of semantic communication," in *2011 IEEE Network Science Workshop*. IEEE, 2011, pp. 110–117.
- [3] J. Dai, S. Wang, K. Tan, Z. Si, X. Qin, K. Niu, and P. Zhang, "Nonlinear transform source-channel coding for semantic communications," *IEEE Journal on Selected Areas in Communications*, vol. 40, no. 8, pp. 2300–2316, 2022.
- [4] M. Yang and H.-S. Kim, "Deep joint source-channel coding for wireless image transmission with adaptive rate control," in *ICASSP 2022-2022 IEEE International Conference on Acoustics, Speech and Signal Processing (ICASSP)*. IEEE, 2022, pp. 5193–5197.
- [5] Y. Sun, H. Chen, X. Xu, P. Zhang, and S. Cui, "Semantic knowledge base-enabled zero-shot multi-level feature transmission optimization," *IEEE Transactions on Wireless Communications*, 2023.
- [6] A. Van Den Oord, O. Vinyals *et al.*, "Neural discrete representation learning," *Advances in neural information processing systems*, vol. 30, 2017.
- [7] M. Nemati and J. Choi, "All-in-one: Vqvae for end-to-end joint source-channel coding," DOI: <https://doi.org/10.36227/techrxiv>, vol. 19294622, p. v1, 2022.
- [8] Q. Fu, H. Xie, Z. Qin, G. Slabaugh, and X. Tao, "Vector quantized semantic communication system," *IEEE Wireless Communications Letters*, 2023.
- [9] L. Guo, W. Chen, Y. Sun, and B. Ai, "Joint device-edge digital semantic communication with adaptive network split and learned non-linear quantization," *arXiv preprint arXiv:2305.13553*, 2023.
- [10] D. Lee, C. Kim, S. Kim, M. Cho, and W.-S. Han, "Autoregressive image generation using residual quantization," in *Proceedings of the IEEE/CVF Conference on Computer Vision and Pattern Recognition*, 2022, pp. 11 523–11 532.
- [11] D. Yang, S. Liu, R. Huang, J. Tian, C. Weng, and Y. Zou, "Hifi-codect: Group-residual vector quantization for high fidelity audio codec," *arXiv preprint arXiv:2305.02765*, 2023.
- [12] P. Esser, R. Rombach, and B. Ommer, "Taming transformers for high-resolution image synthesis," in *Proceedings of the IEEE/CVF conference on computer vision and pattern recognition*, 2021, pp. 12 873–12 883.
- [13] C. Chen, X. Shi, Y. Qin, X. Li, X. Han, T. Yang, and S. Guo, "Real-world blind super-resolution via feature matching with implicit high-resolution priors," in *Proceedings of the 30th ACM International Conference on Multimedia*, 2022, pp. 1329–1338.
- [14] E. Agustsson and R. Timofte, "Ntire 2017 challenge on single image super-resolution: Dataset and study," in *Proceedings of the IEEE conference on computer vision and pattern recognition workshops*, 2017, pp. 126–135.
- [15] B. Lim, S. Son, H. Kim, S. Nah, and K. Mu Lee, "Enhanced deep residual networks for single image super-resolution," in *Proceedings of the IEEE conference on computer vision and pattern recognition workshops*, 2017, pp. 136–144.
- [16] S. Gu, A. Lugmayr, M. Danelljan, M. Fritsche, J. Lamour, and R. Timofte, "Div8k: Diverse 8k resolution image dataset," in *2019 IEEE/CVF International Conference on Computer Vision Workshop (ICCVW)*. IEEE, 2019, pp. 3512–3516.
- [17] T. Karras, T. Aila, S. Laine, and J. Lehtinen, "Progressive growing of gans for improved quality, stability, and variation," *arXiv preprint arXiv:1710.10196*, 2017.
- [18] [Online]. Available: <https://bellard.org/bpg/>.
- [19] G. K. Wallace, "The jpeg still picture compression standard," *Communications of the ACM*, vol. 34, no. 4, pp. 30–44, 1991.
- [20] R. Zhang, P. Isola, A. A. Efros, E. Shechtman, and O. Wang, "The unreasonable effectiveness of deep features as a perceptual metric," in *Proceedings of the IEEE conference on computer vision and pattern recognition*, 2018, pp. 586–595.